Published OnlineFirst May 11, 2020; DOI: 10.1158/1535-7163.MCT-19-0910

Blockade of Cell Volume Regulatory Protein NKCC1 Increases TMZ-Induced Glioma Apoptosis and Reduces Astrogliosis

Lanxin Luo[1,2,3], Xiudong Guan[3,4,5,6,7], Gulnaz Begum[3], Dawei Ding[3], Jenesis Gayden[8], Md Nabiul Hasan[3], Victoria M. Fiesler[3], Jacob Dodelson[3], Gary Kohanbash[9,10], Baoli Hu[9], Nduka M. Amankulor[9], Wang Jia[4,5,6,7], Maria G. Castro[11], Baoshan Sun[2,12], and Dandan Sun[3,13]

ABSTRACT

Glioma is one of the most common primary malignant tumors of the central nervous system accounting for approximately 40% of all intracranial tumors. Temozolomide is a conventional chemotherapy drug for adjuvant treatment of patients with high-risk gliomas, including grade II to grade IV. Our bioinformatic analysis of The Cancer Genome Atlas and Chinese Glioma Genome Atlas datasets and immunoblotting assay show that *SLC12A2* gene and its encoded Na^+-K^+-$2Cl^-$ cotransporter isoform 1 (NKCC1) protein are abundantly expressed in grade II–IV gliomas. NKCC1 regulates cell volume and intracellular Cl^- concentration, which promotes glioma cell migration, resistance to temozolomide, and tumor-related epilepsy in experimental glioma models. Using mouse syngeneic glioma models with intracranial transplantation of two different glioma cell lines (GL26 and SB28), we show that NKCC1 protein in glioma tumor cells as well as in tumor-associated reactive astrocytes was significantly upregulated in response to temozolomide monotherapy. Combination therapy of temozolomide with the potent NKCC1 inhibitor bumetanide reduced tumor proliferation, potentiated the cytotoxic effects of temozolomide, decreased tumor-associated reactive astrogliosis, and restored astrocytic GLT-1 and GLAST glutamate transporter expression. The combinatorial therapy also led to suppressed tumor growth and prolonged survival of mice bearing GL26 glioma cells. Taken together, these results demonstrate that NKCC1 protein plays multifaceted roles in the pathogenesis of glioma tumors and presents as a therapeutic target for reducing temozolomide-mediated resistance and tumor-associated astrogliosis.

Introduction

The World Health Organization (WHO)-classified low-grade gliomas (LGG) consist of grade I and grade II tumors, while high-grade gliomas (HGG) consist of grade III and grade IV tumors (1). Grade I gliomas, primarily occurring in children, lack classical histopathologic features of tumors, such as atypia, anaplasia, mitotic activity, microvascular proliferation, and necrosis (2, 3) and are frequently curable with complete surgical resection (2). Grade II gliomas, such as astrocytoma and oligodendroglioma (4), are diffuse and their infiltrative intracerebral lesions are rarely curable (5). Grade II gliomas are more epileptogenic than HGGs (6) and almost all of the grade II lesions progress to HGGs eventually (2, 7, 8). Among all grades of gliomas, grade II gliomas have an indolent course with longer term survival (~7 years), compared with grade III gliomas (with median survival around 3 years; ref. 9). Grade IV glioblastoma (GBM) is the most aggressive primary brain tumor with life expectancy of barely 12–15 months from detection, despite of the aggressive standard therapeutic regimens (10, 11).

Na^+-K^+-$2Cl^-$ cotransporter isoform 1 (NKCC1) belongs to the *SLC12A* family of cation-chloride cotransporters, which plays a vital role in regulation of cell volume and intracellular Cl^- concentration (12). Recent studies show the association of NKCC1 protein with gliomas, especially relating to GBM cell migration and invasion (10, 12–15). NKCC1 protein localizes to the leading edge of glioma cells and pharmacologic inhibition or genetic knockdown of NKCC1 inhibits glioma cell volume increase and reduces glioma cell migration in experimental models (13). NKCC1 protein in patient-derived human primary glioma cells is responsible for active intracellular chloride (Cl^-_i) accumulation and functions as the primary mechanism for regulatory volume increase in response to osmotic cell shrinkage (16) or in counteracting apoptotic volume decrease (AVD) mediated by temozolomide-induced apoptosis *in vitro* (16). NKCC1 also modulates migration of cultured human primary GBM cells through the regulation of focal adhesion dynamics and cell contractility (12) or through interacting with ezrin-radixin-moesin (ERM) cytoskeleton proteins (15). Furthermore, analysis of The Cancer Genome Atlas (TCGA) dataset reveals that patients with GBM with

[1]School of Traditional Chinese Materia Medica, Shenyang Pharmaceutical University, Shenyang, Liaoning, China. [2]School of Functional Food and Wine, Shenyang Pharmaceutical University, Shenyang, Liaoning, China. [3]Department of Neurology, University of Pittsburgh, Pittsburgh, Pennsylvania. [4]Department of Neurosurgery, Beijing Tiantan Hospital, Capital Medical University, Beijing, China. [5]Chinese National Clinical Research Center for Neurological Diseases, Beijing, China. [6]Beijing Neurosurgical Institute, Beijing, China. [7]Chinese Glioma Genome Atlas Network, Beijing, China. [8]Center for Neuroscience, University of Pittsburgh, Pittsburgh, Pennsylvania. [9]Department of Neurological Surgery, University of Pittsburgh, Pittsburgh, Pennsylvania. [10]Department of Immunology, University of Pittsburgh, Pittsburgh, Pennsylvania. [11]Department of Neurosurgery and Department of Cell and Developmental Biology, University of Michigan Medical School, Ann Arbor, Michigan. [12]Pólo Dois Portos, Instituto National de Investigação Agrária e Veterinária, I.P., Quinta da Almoinha, Dois Portos, Portugal. [13]Veterans Affairs Pittsburgh Health Care System, Geriatric Research, Educational and Clinical Center, Pittsburgh, Pennsylvania.

Note: Supplementary data for this article are available at Molecular Cancer Therapeutics Online (http://mct.aacrjournals.org/).

Corresponding Authors: Dandan Sun, University of Pittsburgh, Pittsburgh, PA 15260. Phone: 412-624-0418; Fax: 412-648-3321; E-mail: sund@upmc.edu; and Baoshan Sun, Shenyang Pharmaceutical University, 103 Wenhua Road, Shenyang, Liaoning 110016, China. Phone: 86-150-0401-1284; E-mail: sun.baoshan@iniav.pt

Mol Cancer Ther 2020;19:1550–61

doi: 10.1158/1535-7163.MCT-19-0910

Published OnlineFirst May 11, 2020; DOI: 10.1158/1535-7163.MCT-19-0910

high *SLC12A2* mRNA expression had a significantly shorter overall survival (14). These findings strongly indicate that NKCC1 protein likely uses the above signaling mechanisms to regulate glioma migration/invasion and progression. However, impact of blockade of NKCC1 protein function in combination of temozolomide therapy on inhibiting glioma progression has not been examined in animal models of gliomas.

In this study, in two intracranial mouse syngeneic glioma models, temozolomide monotherapy significantly upregulated NKCC1 protein expression in glioma tumor cells as well as in tumor-associated reactive astrocytes. Combination therapy of temozolomide with the potent NKCC1 inhibitor, bumetanide, reduced tumor proliferation, potentiated the cytotoxic effects of temozolomide, decreased tumor-associated reactive astrogliosis, and restored astrocytic GLT-1 and GLAST glutamate transporters expression. The combinatorial therapy also led to suppressed tumor growth and prolonged survival of mice bearing GL26 glioma cells. Our results demonstrate that NKCC1 protein plays multifaceted roles in the pathogenesis of glioma and presents a therapeutic target for reducing tumor-associated reactive astrogliosis and temozolomide resistance.

Materials and Methods

Materials

Bumetanide (catalog no. B3023) and temozolomide (catalog no. T2577) were purchased from Sigma-Aldrich. DMEM (DMEM/HEPES, catalog no. 12430-054) and penicillin/streptavidin (catalog no. 15240062) were from Gibco. FBS and G418 disulfate solution were obtained from Invitrogen. Antibodies used in this work are described in Supplementary Materials and Methods.

Bioinformatic data collection and analysis

Whole-genome mRNA-sequencing data were downloaded from Chinese Glioma Genome Atlas (CGGA) database (http://www.cgga.org.cn), which is generated by Illumina HiSeq platform and approved by Capital Medical University Institutional Review Board (Beijing, China), and from TCGA database (https://portal.gdc.cancer.gov/). Transcriptome sequencing data of 325 glioma samples were downloaded from CGGA and mRNA-sequencing data of 698 gliomas, ranging from WHO grade II to grade IV, were downloaded from public TCGA database. RNA-sequencing data of CGGA (FPKM value) and TCGA (FPKM value) were log transformed before analysis. For the expression analysis, cases were classified into different groups according to WHO grade classification and histologic type (17).

Cell cultures and authentication

Immunogenic mouse glioma GL26 and glioma GL26-mCitrine (GL26-cit) cells and nonimmunogenic mouse SB28-GFP glioma cells were used as described previously (8). Cells were cultured as described previously (18). All cell lines were authenticated by short tandem repeat DNA Fingerprinting (by IDEXX BioResearch) in the past 6 months. In addition, PCR analysis was performed to confirm the absence of *Mycoplasma* infection in all cell cultures.

Human glioma tissue samples

Paraformaldehyde (PFA) fixed tissues and nonfixed fresh tissues from surgically removed central nervous system (CNS) tumors were collected at the Department of Pathology, University of Pittsburgh Medical Center, following approval by the institutional review boards. All tumors were classified according to WHO diagnostic criteria.

Immunoblotting

Immunoblotting of pNKCC1 and tNKCC1 in cell cultures, mouse, and human glioma tissues was performed as described in Supplementary Materials and Methods.

NKCC1-mediated rubidium uptake assay

Glioma cells seeded in 24-well plates (80% confluent) were treated with vehicle (DMSO in PBS), temozolomide (100 μmol/L), bumetanide (10 μmol/L), or temozolomide + bumetanide (T + B) in the culture medium for 48 hours. To measure rubidium (Rb^+) uptake in glioma cells, the culture medium was removed and cells were rinsed with an isotonic washing buffer (310 mOsm, containing 134 mmol/L NaCl, 2 mmol/L $CaCl_2$, 0.8 mmol/L NaH_2PO_4, 5 mmol/L glucose, 25 mmol/L HEPES, and 1.66 mmol/L $MgSO_4$). Cells were exposed to the isotonic buffer containing 5.36 mmol/L Rb^+ in the absence or presence of bumetanide (10 μmol/L) for 15 minutes at 37°C. To measure Rb^+ influx in glioma cells in response to hypertonic stress, cells were exposed to the hypertonic solution (400 mOsm adjusted with 7.7 mmol/L sucrose and 5.36 mmol/L Rb^+) for 15 min at 37°C. To terminate Rb^+ influx, cells were washed with the isotonic or hypertonic washing solutions (Rb^+ free) and lysed with 0.15% SDS (200 μL/well) to release intracellular Rb^+. The intracellular Rb^+ concentration in cell lysates was measured using an automated atomic absorption spectrophotometer (Ion Channel Reader, ICR-8000, Aurora Biomed). Total protein of cell lysates was measured by BCA assay. NKCC1-mediated Rb^+ influx was determined by subtracting Rb^+ influx value in the presence of bumetanide from one in the absence of bumetanide during the 15-minute assay. Rb^+ influx rate was calculated and presented as μg Rb^+/mg protein/minute.

Mouse syngeneic glioma models

All animal experiments were approved by the University of Pittsburgh Institutional Animal Care and Use Committee and performed in accordance with the NIH Guide for the Care and Use of Laboratory Animals.

Implantation of glioma cells in C57BL/6 mice (female, 6–8 weeks old) was described previously (19). Intracranial allografts of GL26-cit mouse glioma cells represent a well-established syngeneic glioma model (19, 20). SB28-GFP is a newly developed mouse cell line, which does not express detectable CD40, and represents a weakly immunogenic glioma model (18, 19).

Animal survival test

Drug treatment regimen for animal survival test was performed as described in Supplementary Materials and Methods. Tumor-bearing mice were monitored daily for signs of pain, discomfort, or neurologic impairment. Signs of chronic pain, such as hunched posture, weight loss, and absence of grooming behavior, and of neurologic impairment, like seizures, weakness, difficulty in walking, an inability to right themselves, circling behavior, and unusual aggressiveness or timidity were used to infer tumor development. A loss of 20% body weight, severe neurologic impairment, or major loss in body scoring index (<2.0 on a 5-point scale) were used as the animal humane end point. All other surviving mice were sacrificed at 90 days after glioma cell injection.

Evaluation of xenograft glioma tumor tissues

At the end of the drug treatments, mice were anesthetized with 3% isoflurane in 70% N_2O and 30% O_2 and exhibited no toe and tail reflexes. Mice were perfused with 0.9% saline solution followed by 4% PFA in PBS (pH 7.4). Mouse brains were harvested and stored in 4%

Published OnlineFirst May 11, 2020; DOI: 10.1158/1535-7163.MCT-19-0910

PFA at 4°C overnight, then stored in 30% sucrose for at least 2 days. Evaluation of tumor volume and invasion is described in Supplementary Materials and Methods.

Immunofluorescence staining

Human glioma brain tissue sections (10 μm) and mouse brain tissue sections (25 μm) were mounted on microscope slides. Immunofluorescence staining for NKCC1, GFAP, GLT-1, and GLAST were performed as described in Supplementary Materials and Materials. The image analysis is further described in Supplementary Materials and Methods.

Morphologic analysis of tumor-associated reactive astrocytes

The detailed description of morphologic analysis of reactive astrocytes (process length, process number, and cell volume) is shown in Supplementary Materials and Methods.

Statistical analysis

The results were expressed as the mean ± SEM. Statistical significance was determined using one-way or two-way ANOVA for multiple comparisons by GraphPad Prism 8 (GraphPad Software, Inc). Mouse survival was evaluated using Kaplan–Meier analysis and compared with a two-sided log-rank test. Data are significant when *, $P < 0.05$; **, $P < 0.01$; ***, $P < 0.001$; and ****, $P < 0.0001$. *N* values represent the number of independent experiments.

Results

SLC12A2 mRNA and NKCC1 protein expression in gliomas

Analysis of the mRNA-sequencing data of both CGGA and TCGA datasets revealed that *SLC12A2* mRNA expression was relatively higher in WHO grade II gliomas than in grade IV gliomas ($P < 0.05$; **Fig. 1A**). According to the histologic types of glioma, the high level of *SLC12A2* mRNA expression was more abundant in oligodendroglioma in TCGA datasets ($P < 0.001$; **Fig. 1B**). Expression of NKCC1 protein in human gliomas was further demonstrated with immunofluorescence staining (eight PFA-fixed glioma tissues) and immunoblotting (sic nonfixed tissues) ranging from grade II to grade IV, respectively. Immunofluorescence staining illustrated that grade II gliomas exhibited relatively higher level of NKCC1 protein expression than grade III/IV ($P < 0.05$; **Fig. 1C**). However, abundant NKCC1 protein expression was detected in grade II–III/IV gliomas with the immunoblotting assay (**Fig. 1D**). Collectively, these findings indicate that NKCC1 protein is abundantly expressed in all grades of glioma tumors and may play an important role in glioma progression.

Temozolomide stimulates NKCC1 protein expression and NKCC1-mediated Rb^+ influx in cultured mouse glioma cells

Figure 2A illustrates cell treatment protocol with subsequent immunoblotting or Rb^+ influx assays. Comparing with the vehicle controls, incubation of GL26 glioma cells with temozolomide for 48 hours triggered increase of phosphorylated NKCC1 (pNKCC1) protein expression by approximately 10.9% ($P > 0.05$) and total NKCC1 protein (tNKCC1) by approximately 31.5% ($P < 0.001$; **Fig. 2C**). Interestingly, temozolomide plus NKCC1 inhibitor bumetanide treatment blocked the temozolomide-induced tNKCC1 ($P < 0.0001$) or pNKCC1 upregulation ($P < 0.05$; **Fig. 2C**). Similar findings were detected in SB28-GFP cells (**Fig. 2B**). The full-length blots of pNKCC1 and tNKCC1 in GL26 and SB28-GFP glioma cells are shown in Supplementary Fig. S1A and S1B. In assessing NKCC1 activity in glioma cells via measuring Rb^+ influx, we found that temozolomide treatment of GL26 cultures for 48 hours significantly stimulated NKCC1-mediated Rb^+ uptake (bumetanide-sensitive Rb^+ influx) under isotonic conditions (~67.8%; $P < 0.0001$; **Fig. 2D** and **E**), which was not further activated by hypertonic osmotic stress (**Fig. 2E**). These findings suggest that temozolomide-induced upregulation and activation of NKCC1 protein is likely via the same mechanism as osmotic shrinkage. GL26 cultures treated with T+B displayed reduced NKCC1-mediated Rb^+ uptake by approximately 34.9% in isotonic conditions ($P < 0.0001$) and by approximately 19.8% in hypertonic conditions ($P < 0.05$; **Fig. 2E**). SB28-GFP cells exhibited similar changes in Rb^+ uptake under above conditions (**Fig. 2F**). These findings clearly demonstrate that temozolomide exposure not only triggers stimulation of NKCC1 protein expression and phosphorylation, but also leads to increase of NKCC1-mediated ionic flux activity. These changes may affect glioma progression *in vivo*.

Temozolomide stimulates NKCC1 protein upregulation in mouse glioma tissues

We further investigated changes of NKCC1 protein expression and its association with glioma pathogenesis in the two mouse syngeneic glioma models. C57BL/6J mice transplanted with GL26-cit or SB28-GFP cells randomly received vehicle control (DMSO), temozolomide, bumetanide, or T + B regimens for 5 consecutive days (**Fig. 3A**). Low tNKCC1 protein expression was detected in GL26-cit tumors in the vehicle-treated control mice (arrowhead, **Fig. 3B**). Mice treated with temozolomide displayed increased tNKCC1 protein by approximately 78.4% ($P < 0.0001$), about 62.7% of the tNKCC1 protein immunoreactive signals were colocalized with GL26-cit fluorescence ($P < 0.0001$; **Fig. 3B**), implying an upregulation of NKCC1 protein in glioma tumor cells. In contrast, bumetanide monotherapy did not significantly affect tNKCC1 protein expression in GL26-cit tumors (**Fig. 3B**). Consistent with our *in vitro* study findings, no upregulation of tNKCC1 protein was detected in mice treated with the T+B combination regimen (**Fig. 3B**). Mice bearing SB28-GFP tumors exhibited similar patterns of tNKCC1 protein expression under the four treatment regimens (**Fig. 3C**). To strengthen our conclusion, we also performed immunoblotting analysis for changes of NKCC1 protein expression in the GL26-cit mouse glioma tissues under different treatment regimens (vehicle, temozolomide, bumetanide, or T+B; Supplementary Fig. S2). Low tNKCC1 protein expression was detected in GL26-cit tumors in the vehicle-treated control mice. Mice treated with temozolomide displayed increased tNKCC1 protein by approximately 185% ($P < 0.001$; Supplementary Fig. S2). Bumetanide monotherapy did not affect tNKCC1 protein expression in the GL26-cit tumors (Supplementary Fig. S2). Consistent with immunofluorescence study, no upregulation of tNKCC1 protein was detected in mice treated with the T+B combination therapy (Supplementary Fig. S2). We also detected temozolomide-induced upregulation of tNKCC1 protein in nontumor cells (GL26-cit$^-$; arrow, **Fig. 3B** and **C**), and these were tumor-associated astrocytes, and to be discussed later (**Fig. 5**). In short, our data clearly show that GL26-cit or SB28-GFP glioma tumor cells elevate NKCC1 protein expression in response to temozolomide treatment, and combining pharmacologic inhibition of NKCC1 protein with temozolomide therapy prevented such changes.

Combining temozolomide therapy with NKCC1 blockade reduces glioma proliferation and increases apoptosis in mouse glioma allografts

We further evaluated whether the combination therapy sensitizes tumors to temozolomide-mediated cytotoxicity. The order of tumor volume of GL26-cit or SB28-GFP with four treatment regimens was as

Published OnlineFirst May 11, 2020; DOI: 10.1158/1535-7163.MCT-19-0910

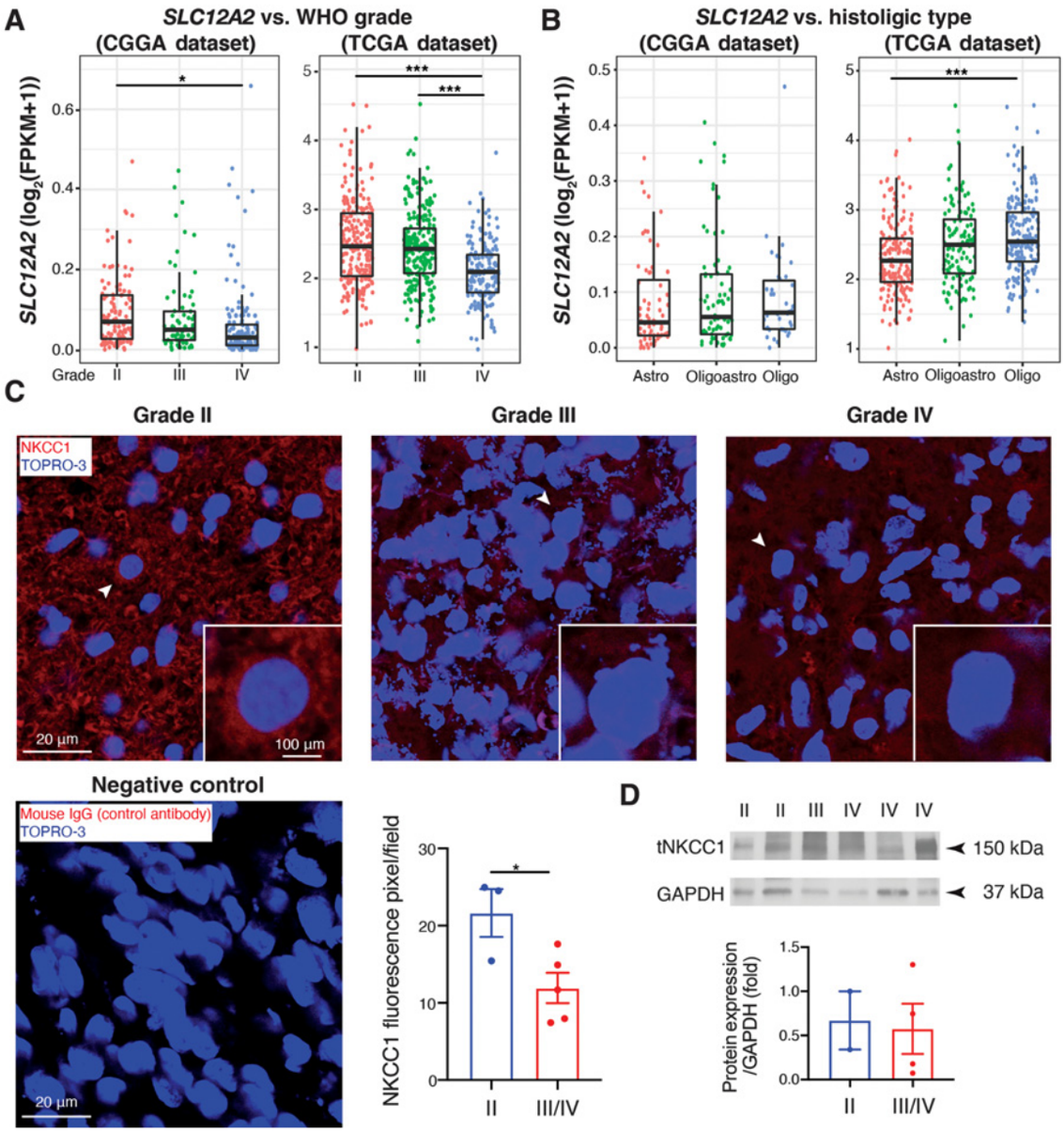

Figure 1.

SLC12A2 mRNA and NKCC1 protein expression in gliomas. **A,** *SLC12A2* mRNA expression in different WHO grade gliomas from CGGA ($n = 325$) and TCGA ($n = 698$) datasets, respectively. Data are means ± SD. *, $P < 0.05$; ***, $P < 0.001$. **B,** *SLC12A2* mRNA expression according to histologic type. Data are mean ± SD. CGGA ($n = 179$) and TCGA ($n = 467$). ***, $P < 0.001$. **C,** NKCC1 protein expression in different WHO grade (II–IV) glioma tissues was determined by immunostaining. Data are means ± SEM ($n = 3$-5); *, $P < 0.05$. **D,** NKCC1 protein expression in different WHO grade (II–IV) glioma tissues was determined by immunoblotting. Data are means ± SEM ($n = 2$–3).

following: vehicle control or bumetanide > temozolomide > T+B. Compared with the vehicle control, combining temozolomide treatment with bumetanide significantly decreased both GL26-cit ($P < 0.01$; **Fig. 4A**) and SB28-GFP glioma growth ($P < 0.001$; Supplementary Fig. S3A). We then evaluated changes of tumor invasion by measuring the maximal invasion distance (starting from the tumor center) and the invasive front area. Temozolomide or bumetanide monotherapy did not reduce tumor invasion distance nor area in the GL26-cit tumors, compared with the vehicle control (**Fig. 4B**). However, the T+B combination therapy reduced the tumor invasion distance by approximately 49 % and area by approximately 28 %, respectively ($P < 0.0001$; **Fig. 4B**). The same results were detected in SB28-GFP tumor–bearing mice (supplementary Fig. 4B). We anticipate that changes of tumor proliferation and apoptosis are involved in the tumor volume reduction. The immunoreactive intensity of Ki67, a marker for activated cell cycle (21), was high in the GL26-cit tumor cells in the vehicle-treated control mice (**Fig. 4C**). Bumetanide or temozolomide monotherapy did not change the number of $Ki67^+$

Published OnlineFirst May 11, 2020; DOI: 10.1158/1535-7163.MCT-19-0910

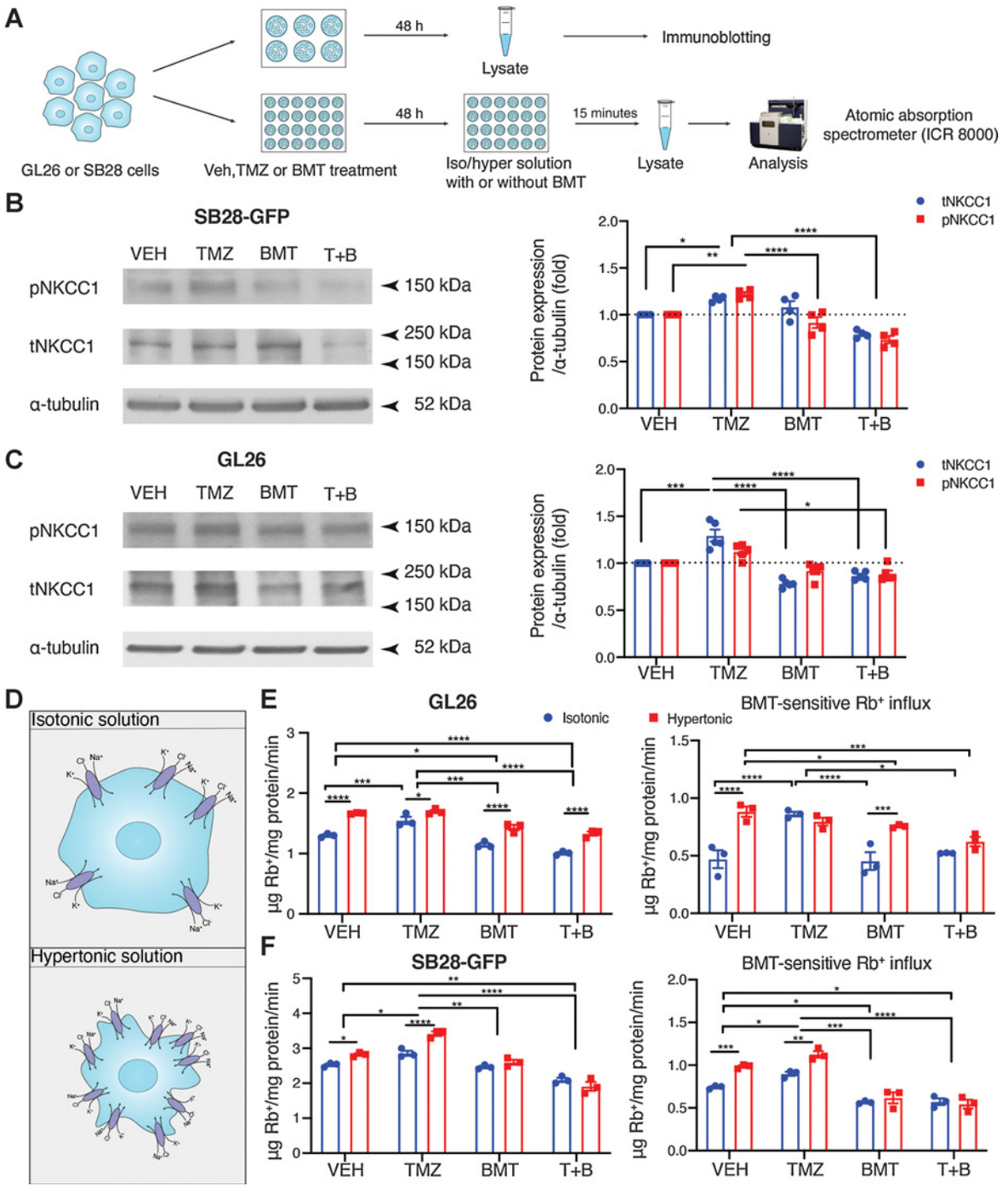

Figure 2.

Temozolomide (TMZ) stimulates NKCC1 protein expression and activity in cultured glioma cells. **A,** Experimental protocol of immunoblotting and Rb^+ influx assays. **B,** SB28-GFP cells were exposed to temozolomide (100 μmol/L), bumetanide (BMT, 10 μmol/L), or T+B combined for 48 hours and cell lysates were harvested for immunoblotting. Total NKCC1 protein (tNKCC1) or phosphorylated NKCC1 (pThr206) were probed. Data are means ± SEM ($n = 4$); *, $P < 0.05$; **, $P < 0.01$; ****, $P < 0.0001$. **C,** GL26 cells were exposed to temozolomide, bumetanide, or T+B combined as in **B**. Data are means ± SEM ($n = 5$); *, $P < 0.05$; ***, $P < 0.001$; ****, $P < 0.0001$. **D,** Schematic model of NKCC1 function in tumor cells in response to isotonic and hypertonic solutions. **E,** GL26 cells were exposed to temozolomide, bumetanide, or T+B combined for 48 hours. Rb^+ influx into cells under either isotonic (15 minutes, 310 mOsm) or hypertonic (15 minutes, 400 mOsm) solutions was determined using ICR 8000. Either total or NKCC1-mediated Rb^+ influx (as bumetanide-sensitive Rb^+ influx) was displayed. Data are means ± SEM ($n = 3$); *, $P < 0.05$; ***, $P < 0.001$; ****, $P < 0.0001$. **F,** SB28-GFP cells were exposed to temozolomide, bumetanide, or T+B combined as in **E**. Data are means ± SEM ($n = 3$; *, $P < 0.05$; **, $P < 0.01$; ***, $P < 0.001$; ****, $P < 0.0001$). Veh, vehicle.

Published OnlineFirst May 11, 2020; DOI: 10.1158/1535-7163.MCT-19-0910

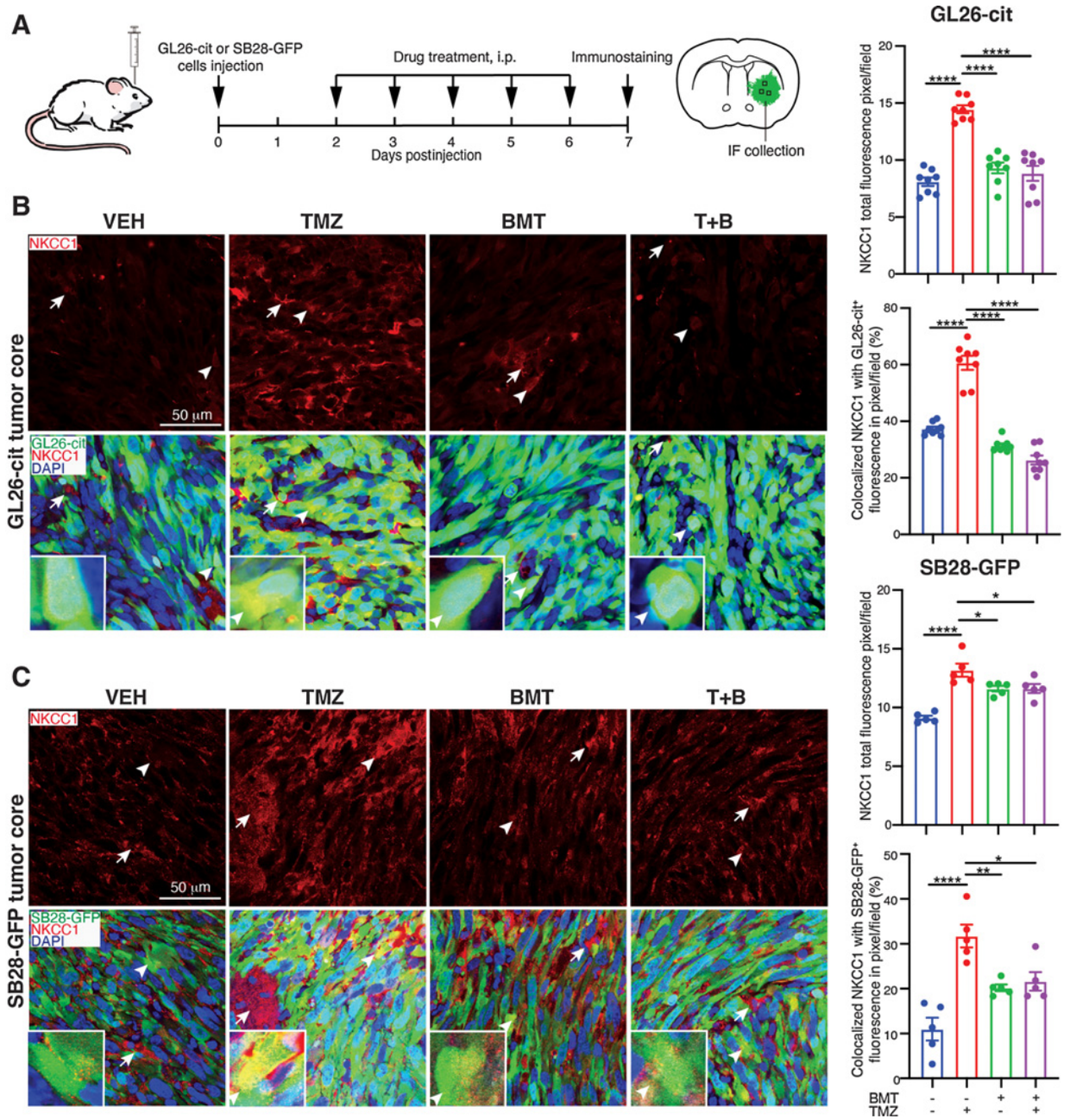

Figure 3.

Temozolomide (TMZ) stimulates NKCC1 expression in glioma tissues. **A,** Experimental protocol and data collection. GL26-cit cells (40,000) or SB28-GFP cells (50,000) were injected in the right striatum of C57BL6/J mice. Starting 2 d.p.i., mice received intraperitoneal injections (i.p.) of either vehicle PBS-DMSO, temozolomide (2.5 mg/kg/day), bumetanide (BMT, 5 mg/kg/twice a day), or T+B combination (2.5 mg/kg/day, 5 mg/kg/twice a day) for 5 consecutive days. Mice were sacrificed at 7 d.p.i. and fixed brain sections (25 μm) were used for immunofluorescence staining (IF). **B,** Representative immunostaining images of tNKCC1 protein expression in GL26-Cit tumors. Data are means ± SEM ($n = 8$); ****, $P < 0.0001$. **C,** Representative immunostaining images of tNKCC1 protein expression in SB28-GFP tumors. Data are means ± SEM ($n = 5$; *, $P < 0.05$; **, $P < 0.01$; ****, $P < 0.0001$). VEH, vehicle.

tumor cells, compared with the vehicle control group. However, the T+B combination regimen in GL26-cit mice significantly reduced $Ki67^+$ tumor cells ($P < 0.0001$; **Fig. 4C**). An identical pattern of the changes in $Ki67^+$ cells was detected in the SB28-GFP glioma tumors (Supplementary Fig. S3C). For tumor apoptosis, temozolomide and bumetanide treatment alone did not change the number of cleaved caspase-3^+ cells (**Fig. 4D**; Supplementary Fig. S3D). In contrast, combining temozolomide with bumetanide significantly enhanced caspase-3 cleavage activation in GL26-cit and SB28-GFP glioma tumors ($P < 0.001$; **Fig. 4D**; Supplementary Fig. S3D). These results

Published OnlineFirst May 11, 2020; DOI: 10.1158/1535-7163.MCT-19-0910

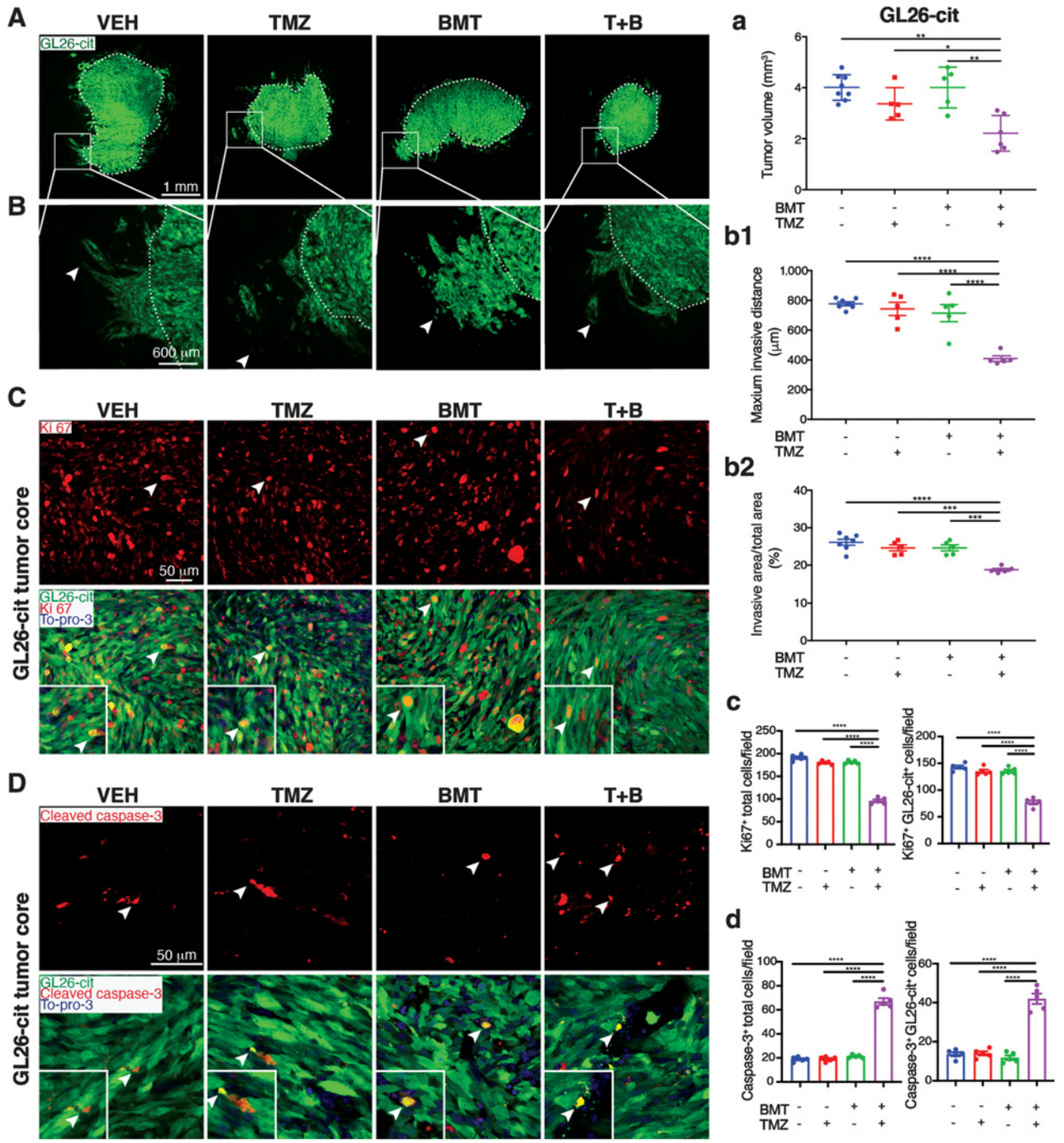

Figure 4.

Combining temozolomide (TMZ) therapy with pharmacologic inhibition of NKCC1 enhances apoptosis and reduces GL26-cit glioma growth. **A,** GL26-cit tumor growth in the same cohort of mice described in **Fig. 3**. Data are means ± SEM ($n = 5$–8) in **A** (**a**), *, $P < 0.05$; **, $P < 0.01$. **B,** Tumor invasion. The maximal invasion distance (**b1**) and invasive area (**b2**) were determined. Data are means ± SEM ($n = 5$–7); ***, $P < 0.001$; ****, $P < 0.0001$. **C,** Total Ki67$^+$ cell counts or Ki67$^+$/GL26-cit$^+$ (**c**) were analyzed. Data are means ± SEM ($n = 5$); ****, $P < 0.0001$. **D,** Total cleaved caspase-3$^+$ apoptotic cell counts or cleaved caspase3$^+$/GL26-cit$^+$ cell counts (**d**) were determined. Data are means ± SEM ($n = 5$; ****, $P < 0.0001$). BMT, bumetanide; Veh, vehicle.

clearly demonstrate that the combination therapy with NKCC1 inhibitor bumetanide accelerates temozolomide-induced apoptosis and inhibits tumor growth in mouse intracranial syngeneic models of glioma.

NKCC1 blockade in combination with temozolomide reduces tumor-associated astrogliosis

We further analyzed NKCC1 protein upregulation in tumor-associated reactive astrocytes. We first detected high colocalization

Published OnlineFirst May 11, 2020; DOI: 10.1158/1535-7163.MCT-19-0910

of NKCC1 protein and GFAP protein in reactive astrocytes adjacent to the peri-tumor regions of GL26-cit tumors (**Fig. 5A–C**). We then assessed the morphologic features of $GFAP^+$ reactive astrocytes of the vehicle control tumors, including process length, number, and cell volume, in three peri-tumor regions (layer 1–3; Supplementary Fig. S4A–S4D). Nontumor normal cortical tissues of the vehicle

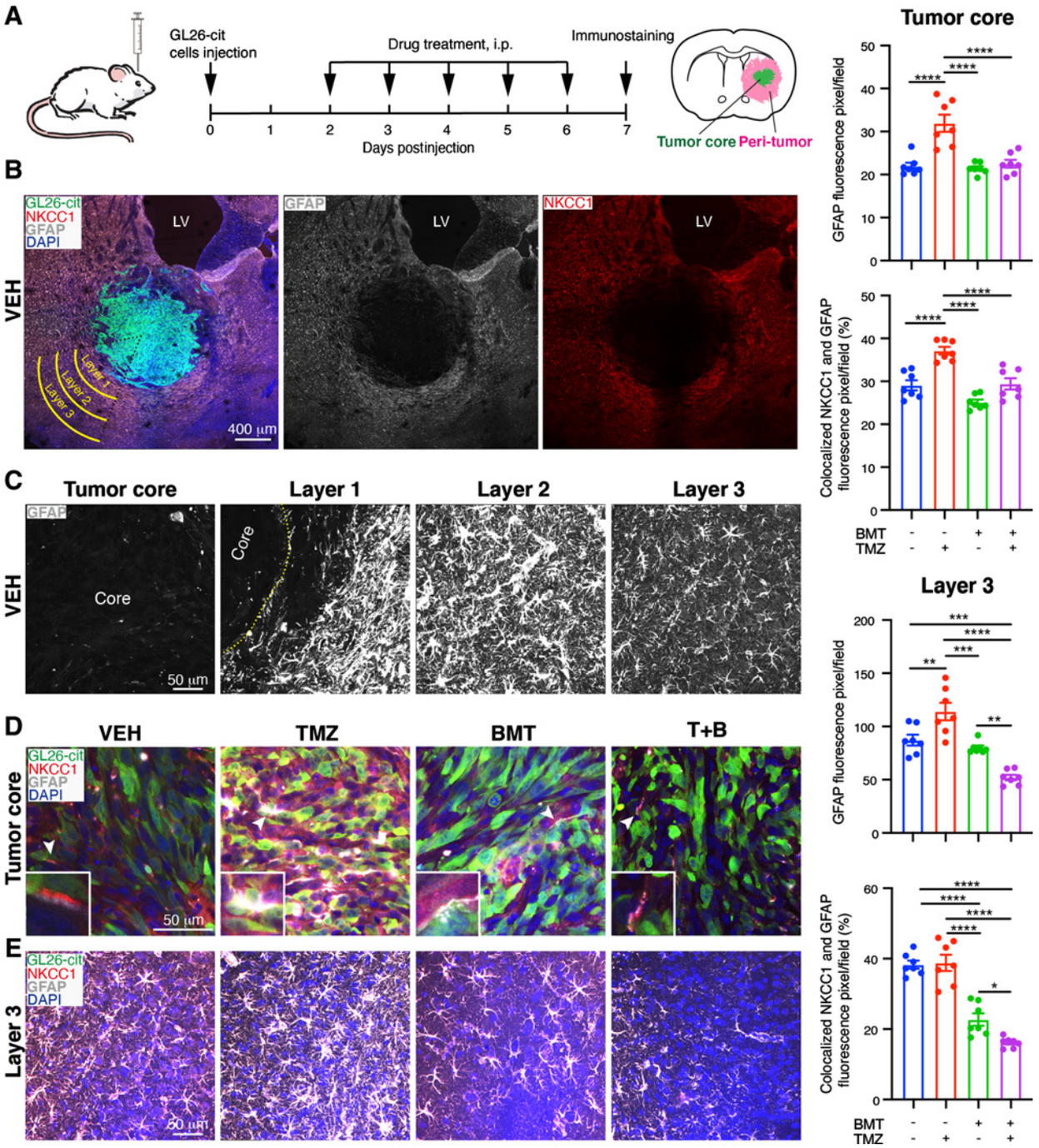

Figure 5.

Combining temozolomide (TMZ) therapy with pharmacologic inhibition of NKCC1 reduces tumor-associated reactive astrogliosis. **A,** Experimental protocol and location of data collection. **B,** Representative immunostaining for GFAP and tNKCC1 protein expression in vehicle (VEH) control GL26-cit mice. **C,** Representative immunostaining for GFAP expression in tumor core and three different layers of peri-tumor regions. **D,** Representative immunostaining for GFAP and tNKCC1 protein expression in GL26-cit tumor core. Data are means ± SEM ($n = 7$); ****, $P < 0.0001$. **E,** Representative immunostaining for GFAP and tNKCC1 protein expression in the GL26-cit peri-tumor layer 3. Data are means ± SEM ($n = 7$; **, $P < 0.01$; ***, $P < 0.001$; ****, $P < 0.0001$). BMT, bumetanide; i.p., intraperitoneal; Veh, vehicle.

Published OnlineFirst May 11, 2020; DOI: 10.1158/1535-7163.MCT-19-0910

control mice were used for nonreactive astrocyte controls (Supplementary Fig. S4A–S4D). GFAP$^+$ astrocytes' volume, mean process length, and number in nontumor normal tissues were low, which are consistent with the literatures (22, 23). However, GFAP$^+$ reactive astrocytes in the peri-tumor layer 1 and 2 displayed highly ramified morphology with increase in cell volume, mean process length, and process numbers (Supplementary Fig. S4A–S4D). GFAP$^+$ reactive astrocytes in the peri-tumor layer 3 showed most significant reduction of ramified morphology with smaller cell volume ($P < 0.05$) and reduced process number, and slightly longer processes than layer 1 and 2 ($P < 0.05$; Supplementary Fig. S4A–S4D).

We next examined NKCC1 protein expression in association with GFAP$^+$ astrogliosis in response to different treatment regimens. Temozolomide monotreatment significantly increased GFAP$^+$ intensity in the GL26-cit tumor core ($P < 0.0001$), which are accompanied with upregulated NKCC1 expression in reactive astrocytes ($P < 0.0001$; **Fig. 5D**). GFAP expression in GL26-cit tumors was positively correlated with NKCC1 protein expression in reactive astrocytes (Pearson correlation coefficient $r = 0.977$; $P < 0.001$). T+B combination therapy prevented upregulation of either GFAP or NKCC1 expression in reactive astrocytes in the GL26-cit tumor core (**Fig. 5D**). In the peri-tumor layer 3, temozolomide significantly increased GFAP protein expression ($P < 0.01$; **Fig. 5E**), but not accompanied with upregulated NKCC1 ($P > 0.05$; **Fig. 5E**). Bumetanide monotherapy did not affect GFAP or NKCC1 protein expression. However, the T+B combinatorial therapy significantly downregulated both GFAP protein and NKCC1 protein expression in layer 3 of GL26-cit tumors ($P < 0.05$; **Fig. 5E**). No downregulation in protein expression of GFAP and NKCC1 was found in immunodeficient SB28-GFP tumors in response to four different treatment (Supplementary Fig. S5). Moreover, detailed quantification of changes of reactive astrocyte morphology in the peri-tumor layer 3 in response to four different treatments in GL26-cit mice are shown in Supplementary Fig. S4E–S4H. T+B combination therapy significantly reduced GFAP$^+$ astrocyte volume ($P < 0.05$) and number of processes ($P < 0.05$), compared with three single treatments (Supplementary Fig. S4E–S4H). Taken together, these findings indicate that combining temozolomide with bumetanide decreases reactive astrocyte formation both in the tumor core and peri-tumor regions.

Combined temozolomide treatment with NKCC1 inhibition upregulates GLT-1 and GLAST glutamate transporters in tumor-associated reactive astrocytes

We then investigated the impact of the combinatorial therapy on changes of GLT-1 and GLAST glutamate transporters in tumor-associated reactive astrocytes. Temozolomide monotherapy did not change astrocytic GLT-1 or GLAST immunoreactive intensity in GL26-cit tumor core or in the peri-tumor layers (**Fig. 6A** and **B**; Supplementary Fig. S6). However, inhibition of NKCC1 with bumetanide increased astrocytic GLT-1 protein expression in tumor core ($P < 0.05$; **Fig. 6A** and **B**) and upregulated GLAST protein expression in the peri-tumor layer 3 ($P < 0.001$; Supplementary Fig. S6). Interestingly, the combinatory therapy of T+B further upregulated astrocytic GLT-1 and GLAST protein expression in both tumor core and peri-tumor layers ($P < 0.001$; **Fig. 6A** and **B**; Supplementary Fig. S6). Our data strongly suggest that NKCC1 blockade in combination with temozolomide treatment restores glutamate uptake transporter expression in peri-tumor astrocytes, which may reduce excitotoxicity and incidence of tumor-related epilepsy by stimulating glutamate transporter–mediated glutamate uptake.

Combining blockade of NKCC1 with temozolomide therapy significantly increases survival of glioma-bearing animals

Finally, we assessed whether blockade of NKCC1 protein could impact animal survival. A cohort of mice were randomly assigned for the mono or combinatorial treatment regimens and monitored until they reached the humane endpoint (**Fig. 6C**). In the case of one cycle treatment regimen (**Fig. 6D**), the vehicle control group exhibited low median survival period (~ 35.5 days; **Fig. 6D**). Temozolomide monotherapy significantly increased median survival to approximately 49 days ($P < 0.001$), but NKCC1 inhibitor bumetanide therapy did not have any effects (~ 34 days; **Fig. 6D**). However, the one cycle T+B combination therapy markedly enhanced median survival to approximately 60 days ($P < 0.01$; **Fig. 6D**). In the case of three cycles of temozolomide and two cycles of bumetanide treatment regimen, the combinatorial therapy further extended the median survival to approximately 66 days ($P < 0.01$) with approximately 30% mice survived for 90 days after implantation (d.p.i.; **Fig. 6D**). The two cycles of bumetanide monotherapy did not change the median survival, but approximately 30% mice also survived for 90 days (**Fig. 6D**). Taken together, these findings suggest that combining NKCC1 blockade with temozolomide therapy improves temozolomide therapy in elongating survival in a well-established mouse syngeneic glioma model.

Discussion

SLC12A2 mRNA and NKCC1 protein expression in gliomas

A major cellular function of NKCC1 protein in normal cells is to maintain K^+ and Cl^- concentration and cell volume homeostasis (24). New reports recently revealed abundant expression of NKCC1 protein in various types of cancer cells, such as gastric cancer cells (25), prostate cancer cells (26), lung adenocarcinoma cells (27), esophageal squamous carcinoma cells (28), and brain tumor cells (29), which is associated with tumor cell proliferation, migration, and invasion. Garzon-Muvdi and colleagues characterized NKCC1 expression in a tissue microarray containing grade II–IV tumors (grade II, $n = 20$; grade III, $n = 21$; and grade IV, $n = 19$), which showed that NKCC1 protein expression was significantly higher in grade IV and grade III tissue samples, compared with grade II tumors (12). Clinical data analysis of TCGA also showed that high levels of *SLC12A2* mRNA expression in tumor cells are associated with poor prognosis outcome in patients with GBM as well as in patients with EGFR-mutated adenocarcinoma (14, 27). In our study, analyzing *SLC12A2* mRNA expression in different grade gliomas from two independent datasets (CGGA and TCGA) show that grade II gliomas displayed relatively higher levels of *SLC12A2* mRNA expression than grade IV. However, abundant NKCC1 protein expression was detected in grade II–III/IV gliomas, revealing NKCC1 was abundantly expressed in all glioma tissues. Considering discrepancies among these different assessments (bioinformatic analysis, immunostaining, and immunoblotting), and the small sample size of human glioma tissues in our immunostaining and immunoblotting analyses, future study with larger sample size of different grades of human gliomas is needed to investigate correlations between NKCC1 protein expression and clinical outcomes.

Effects of combination of temozolomide therapy with NKCC1 blockade on reducing tumor growth

In our experimental glioma models, we detected upregulated NKCC1 protein expression in glioma in response to temozolomide treatment. Temozolomide is known to trigger loss of intracellular

Published OnlineFirst May 11, 2020; DOI: 10.1158/1535-7163.MCT-19-0910

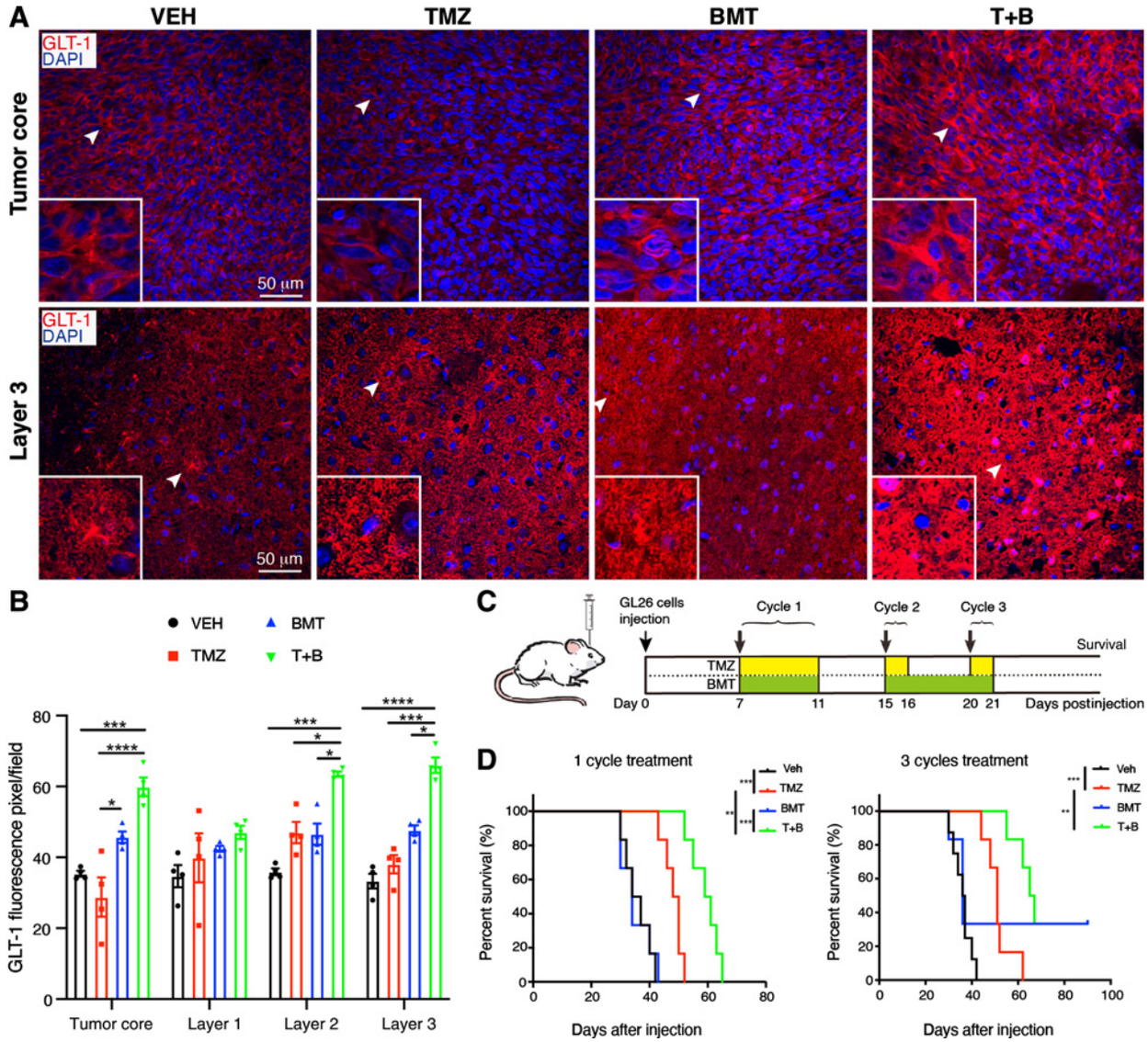

Figure 6.

Combining temozolomide (TMZ) therapy with pharmacologic inhibition of NKCC1 upregulates GLT-1 glutamate transporter in tumor-associated reactive astrocytes and increases GL26 glioma-bearing mouse survival. **A,** Representative immunostaining for GLT-1 protein expression in GL26-cit tumor core and peri-tumor layer 3. **B,** Data are means ± SEM ($n = 4$); *, $P < 0.05$; ***, $P < 0.001$; ****, $P < 0.0001$. **C,** Experimental protocol. Glioma cells were injected into the right striatum of C57BL6/J mice. Starting 7 d.p.i., mice received vehicle PBS-DMSO, temozolomide (50 mg/kg/day, i.p.), bumetanide (BMT, 5 mg/kg, twice a day, i.p.), or T+B combination treatments (50 mg/kg/day, 5 mg/kg twice a day, i.p.) for 5 days for one cycle or three cycles (with two additional 2-day temozolomide treatments). **D,** Kaplan–Meier survival curve of GL26 tumor-bearing mice (each group $n = 5$–7; **, $P < 0.01$; ***, $P < 0.001$). Veh, vehicle.

K^+, Cl^-, and AVD, leading to apoptotic glioma cell death (16). In this process, NKCC1 activity is stimulated through the Cl^-/volume-sensitive regulatory kinases WNK-mediated signaling pathway counteracting ionic dysregulation and AVD in promoting cell survival. Inhibition of temozolomide-induced upregulation of NKCC1 activity with bumetanide can further facilitate loss of intracellular K^+, Cl^-, and AVD, thus accelerating temozolomide-mediated apoptosis in glioma (16). In this study, we detected concurrent temozolomide-induced NKCC1 protein expression, phosphor-stimulation of NKCC1 (elevated pNKCC1 expression), and increased NKCC1-mediated Rb^+ (K^+) influx in glioma cells *in vitro* and *in vivo*. Using the two syngeneic glioma mouse models, we found that combination therapy T + B reduced NKCC1 protein expression, decreased tumor proliferation, enhanced temozolomide-mediated apoptosis, and significantly reduced the tumor volume. Our findings are consistent with recent reports that NKCC1 plays an essential role in proliferation of cultured esophageal squamous cell carcinoma (28), gastric cancer cells (25), and prostatic cancer cells (26) by accelerating cell-cycle progression, such as G_2–M-, G_0–G_1-state. These findings suggest that blockade of NKCC1 activity plus temozolomide therapy presents a novel therapeutic strategy for glioma.

Published OnlineFirst May 11, 2020; DOI: 10.1158/1535-7163.MCT-19-0910

Combination therapy reduced tumor-associated astrogliosis and increased astrocytic glutamate transporter expression

Glioma cells stimulate normal astrocytes into tumor-associated astrocytes via secretion of secretory proteins and extracellular vesicles (30). Tumor-associated astrocytes are involved in tumor cell proliferation, invasion, apoptosis evasion, immunoprotection, and chemoprotection by releasing different cytokines, such as TGFβ1, IL6, and IL8 (31). During tumorigenesis, astrocytes undergo a number of molecular, cellular, and functional changes such as hypertrophic cytoplasmic process and upregulation of cytoskeletal protein GFAP to form reactive astrocytes which is called astrogliosis (32–34). These changes initially aim to aid repairing the healthy tissue and fight the progression of tumor, however, the same mechanisms might as well support tumor growth under the influence of glioma cells (31). In this study, we found increased expression of $GFAP^+$ cells in tumor core and peri-tumor regions in response to temozolomide. Temozolomide also upregulated NKCC1 protein expression in tumor-associated $GFAP^+$ reactive astrocytes in tumor core but not in the peri-tumor regions. However, combining NKCC1 blockade with temozolomide therapy prevented upregulation of astrocytic NKCC1 protein expression and concurrently suppressed tumor-associated reactive astrogliosis in GL26-cit tumor. These findings suggest that astrocytic NKCC1 activation may be a potent mechanism in stimulating tumor-associated astrogliosis.

Reactive astrocytes surrounding the tumor could be involved in seizures (35), which is termed tumor-related epilepsy. Tumor-related epilepsy is primarily found in LGGs with incidence ranged from 60% to 100% (36) but the exact mechanism is unclear and likely to be multifactorial and varied among different tumor types (37). Astrocytes are responsible for the removal of extracellular glutamate through glutamate transporters, including GLAST/EAAT1 and GLT-1/EAAT2, driven by the electrochemical ion gradient such as Na^+, K^+, and Cl^- (35). The GLT-1/EAAT2 is responsible for the reuptake of more than 90% glutamate in the CNS (38). Growing evidence has shown that downregulation of expression and function of astrocytic GLAST/GLT-1 leads to high levels of extracellular glutamate and excitotoxicity (39). Increased glutamate release and neuronal hyperexcitability were detected in the peri-tumoral region, generating seizure activity in glioma-bearing immunodeficient mouse model (37, 40). High levels of extracellular glutamate are also known to increase glioma cell invasion, migration, and growth (41). NKCC1 protein expression in neurons has been suggested to play a role in developing epilepsy or tumor-related epilepsy in glioma (36, 42, 43). Our study showed increased NKCC1 protein expression in tumor-associated reactive astrocytes. Temozolomide treatment further stimulated astrocytic NKCC1 expression in glioma tumor core. Astrocytic GLT-1/GLAST expression was significantly reduced in the tumor core and peri-tumor regions of the vehicle or temozolomide-treated GL26 glioma mice. However, NKCC1 blockade plus temozolomide combinatorial therapy decreased astrocytic NKCC1 expression, but restored astrocytic GLT-1/GLAST expression in both tumor core and peri-tumor regions in GL26 glioma model. Recent report shows that dysregulated astrocytic Cl^- accumulation by NKCC1 impairs glutamate transporter function and astrocytic volume regulation and induces astrocytic swelling, perturbs normal synaptic transmission (44). These findings collectively suggest that inhibition of NKCC1 function may be a new strategy for therapeutic intervention for glioma-associated epilepsy. However, the exact mechanisms for NKCC1 protein in regulating astrocytic GLT-1/GLAST expression are unknown and warrant additional study.

In summary, we report here that temozolomide monotherapy increases the expression of cytoprotective protein NKCC1 in glioma cells and tumor-associated reactive astrocytes. Combining temozolomide therapy with NKCC1 inhibitor enhances temozolomide-induced glioma apoptosis and reduces proliferation and tumor growth. Combining inhibition of NKCC1 with temozolomide also reduced tumor-associated astrocyte formation, recovered astrocytic GLT-1/GLAST glutamate transporter expression, and extended the median survival in the immunogenic GL26 mouse glioma model (Supplementary Fig. S7). Our findings suggest that NKCC1 protein plays multifaceted roles in the pathogenesis of gliomas and presents as a therapeutic target for reducing temozolomide-mediated resistance and tumor-associated astrogliosis.

Disclosure of Potential Conflicts of Interest

No potential conflicts of interest were disclosed.

Authors' Contributions

Conception and design: L. Luo, D. Sun
Development of methodology: L. Luo, X. Guan, G. Begum, V.M. Fiesler, J. Dodelson, G. Kohanbash, M.G. Castro
Acquisition of data (provided animals, acquired and managed patients, provided facilities, etc.): L. Luo, X. Guan, G. Begum, N. Hasan, V.M. Fiesler
Analysis and interpretation of data (e.g., statistical analysis, biostatistics, computational analysis): L. Luo, X. Guan, D. Ding, J. Gayden, N. Hasan, V.M. Fiesler, G. Kohanbash, D. Sun
Writing, review, and/or revision of the manuscript: L. Luo, X. Guan, D. Ding, J. Gayden, N. Hasan, G. Kohanbash, B. Hu, M.G. Castro, B. Sun, D. Sun
Administrative, technical, or material support (i.e., reporting or organizing data, constructing databases): L. Luo, D. Ding, G. Kohanbash, N.M. Amankulor
Study supervision: W. Jia, D. Sun

Acknowledgments

This study was, in part, supported by University of Pittsburgh Medical Center Endowed Chair Professorship and Department of Neurology start-up fund (to D. Sun) and China Scholarship Council (to L. Luo). We thank the Center for Biologic Imaging, University of Pittsburgh for supplying the image analysis software (IMARIS) used in this study.

The costs of publication of this article were defrayed in part by the payment of page charges. This article must therefore be hereby marked *advertisement* in accordance with 18 U.S.C. Section 1734 solely to indicate this fact.

Received September 19, 2019; revised January 29, 2020; accepted May 4, 2020; published first May 11, 2020.

References

1. Louis DN, Perry A, Reifenberger G, von Deimling A, Figarella-Branger D, Cavenee WK, et al. The 2016 World Health Organization classification of tumors of the central nervous system: a summary. Acta Neuropathol 2016; 131:803–20.
2. Claus EB, Walsh KM, Wiencke JK, Molinaro AM, Wiemels JL, Schildkraut JM, et al. Survival and low-grade glioma: the emergence of genetic information. Neurosurgical Focus 2015;38:E6.
3. Delgado-Lopez PD, Corrales-Garcia EM, Martino J, Lastra-Aras E, Duenas-Polo MT. Diffuse low-grade glioma: a review on the new molecular classification, natural history and current management strategies. Clin Transl Oncol 2017;19: 931–44.
4. Sepulveda-Sanchez JM, Munoz Langa J, Arraez MA, Fuster J, Hernandez Lain A, Reynes G, et al. SEOM clinical guideline of diagnosis and management of low-grade glioma (2017). Clin Transl Oncol 2018;20:3–15.

Published OnlineFirst May 11, 2020; DOI: 10.1158/1535-7163.MCT-19-0910

5. Forst DA, Nahed BV, Loeffler JS, Batchelor TT. Low-grade gliomas. Oncologist 2014;19:403–13.
6. Chen DY, Chen CC, Crawford JR, Wang SG. Tumor-related epilepsy: epidemiology, pathogenesis and management. J Neurooncol 2018;139:13–21.
7. Duffau H, Taillandier L. New concepts in the management of diffuse low-grade glioma: proposal of a multistage and individualized therapeutic approach. Neuro Oncol 2015;17:332–42.
8. Kohanbash G, Carrera DA, Shrivastav S, Ahn BJ, Jahan N, Mazor T, et al. Isocitrate dehydrogenase mutations suppress STAT1 and CD8+ T cell accumulation in gliomas. J Clin Invest 2017;127:1425–37.
9. Dong XZ, Noorbakhsh A, Hirshman BR, Zhou TZ, Tang JA, Chang DC, et al. Survival trends of grade I, II, and III astrocytoma patients and associated clinical practice patterns between 1999 and 2010: a SEER-based analysis. Neurooncol Pract 2016;3:29–38.
10. Schiapparelli P, Guerrero-Cazares H, Magana-Maldonado R, Hamilla SM, Ganaha S, Fernandes EGL, et al. NKCC1 regulates migration ability of glioblastoma cells by modulation of actin dynamics and interacting with cofilin. Ebiomedicine 2017;21:94–103.
11. Mukherjee S, Fried A, Hussaini R, White R, Baidoo J, Yalamanchi S, et al. Phytosomal curcumin causes natural killer cell-dependent repolarization of glioblastoma (GBM) tumor-associated microglia/macrophages and elimination of GBM and GBM stem cells. J Exp Clin Cancer Res 2018;37:168.
12. Garzon-Muvdi T, Schiapparelli P, ap Rhys C, Guerrero-Cazares H, Smith C, Kim DH, et al. Regulation of brain tumor dispersal by NKCC1 through a novel role in focal adhesion regulation. PLoS Biol 2012;10:e1001320.
13. Haas BR, Sontheimer H. Inhibition of the sodium-potassium-chloride cotransporter isoform-1 reduces glioma invasion. Cancer Res 2010;70:5597–606.
14. Ma HW, Li T, Tao ZN, Hai L, Tong LQ, Yi L, et al. NKCC1 promotes EMT-like process in GBM via RhoA and Rac1 signaling pathways. J Cell Physiol 2019;234:1630–42.
15. Zhu W, Begum G, Pointer K, Clark PA, Yang SS, Lin SH, et al. WNK1-OSR1 kinase-mediated phospho-activation of Na+-K+-2Cl- cotransporter facilitates glioma migration. Mol Cancer 2014;13:31.
16. Algharabli J, Kintner DB, Wang QW, Begum G, Clark PA, Yang SS, et al. Inhibition of Na(+)-K(+)-2Cl(-) cotransporter isoform 1 accelerates temozolomide-mediated apoptosis in glioblastoma cancer cells. Cell Physiol Biochem 2012;30:33–48.
17. Yan W, Zhang W, You G, Zhang J, Han L, Bao Z, et al. Molecular classification of gliomas based on whole genome gene expression: a systematic report of 225 samples from the Chinese glioma cooperative group. Neuro Oncol 2012;14:1432–40.
18. Kosaka A, Ohkuri T, Okada H. Combination of an agonistic anti-CD40 monoclonal antibody and the COX-2 inhibitor celecoxib induces anti-glioma effects by promotion of type-1 immunity in myeloid cells and T-cells. Cancer Immunology Immunotherapy 2014;63:847–57.
19. Guan X, Hasan MN, Begum G, Kohanbash G, Carney KE, Pigott VM, et al. Blockade of Na/H exchanger stimulates glioma tumor immunogenicity and enhances combinatorial TMZ and anti-PD-1 therapy. Cell Death Dis 2018;9:1010.
20. Baker GJ, Yadav VN, Motsch S, Koschmann C, Calinescu AA, Mineharu Y, et al. Mechanisms of glioma formation: iterative perivascular glioma growth and invasion leads to tumor progression, VEGF-independent vascularization, and resistance to antiangiogenic therapy. Neoplasia 2014;16:543–61.
21. Allegranza A, Girlando S, Arrigoni GL, Veronese S, Mauri FA, Gambacorta M, et al. Proliferating cell nuclear antigen expression in central-nervous-system neoplasms. Virchows Arch A Pathol Anat Histopathol 1991;419:417–23.
22. Geisert EE, Yang LJ, Irwin MH. Astrocyte growth, reactivity, and the target of the antiproliferative antibody, TAPA. J Neurosci 1996;16:5478–87.
23. Begum G, Song SS, Wang SX, Zhao HS, Bhuiyan MIH, Li E, et al. Selective knockout of astrocytic Na+/H+ exchanger isoform 1 reduces astrogliosis, BBB damage, infarction, and improves neurological function after ischemic stroke. Glia 2018;66:126–44.
24. Cuddapah VA, Sontheimer H. Ion channels and tranporters in cancer. 2. Ion channels and the control of cancer cell migration. Am J Physiol Cell Physiol 2011;301:C541–C9.
25. Shiozaki A, Miyazaki H, Niisato N, Nakahari T, Iwasaki Y, Itoi H, et al. Furosemide, a blocker of Na+/K+/2Cl- cotransporter, diminishes proliferation of poorly differentiated human gastric cancer cells by affecting G_0–G_1 state. J Physiol Sci 2006;56:401–6.
26. Hiraoka K, Miyazaki H, Niisato N, Iwasaki Y, Kawauchi A, Miki T, et al. Chloride ion modulates cell proliferation of human androgen-independent prostatic cancer cell. Cell Physiol Biochem 2010;25:379–88.
27. Sun PL, Jin Y, Park SY, Kim H, Park E, Jheon S, et al. Expression of Na+-K+-2Cl-cotransporter isoform 1 (NKCC1) predicts poor prognosis in lung adenocarcinoma and EGFR-mutated adenocarcinoma patients. QJM 2016;109:237–44.
28. Shiozaki A, Nako Y, Ichikawa D, Konishi H, Komatsu S, Kubota T, et al. Role of the Na+/K+/2Cl(-) cotransporter NKCC1 in cell cycle progression in human esophageal squamous cell carcinoma. World J Gastroenterol 2014;20:6844–59.
29. Turner KL, Sontheimer H. Cl- and K+ channels and their role in primary brain tumour biology. Philos Trans R Soc Lond B Biol Sci 2014;369:20130095.
30. Yu TF, Wang XF, Zhi TL, Zhang JX, Wang YY, Nie E, et al. Delivery of MGMT mRNA to glioma cells by reactive astrocyte-derived exosomes confers a temozolomide resistance phenotype. Cancer Lett 2018;433:210–20.
31. Brandao M, Simon T, Critchley G, Giamas G. Astrocytes, the rising stars of the glioblastoma microenvironment. Glia 2019;67:779–90.
32. Okolie O, Bago JR, Schmid RS, Irvin DM, Bash RE, Miller CR, et al. Reactive astrocytes potentiate tumor aggressiveness in a murine glioma resection and recurrence model. Neuro Oncol 2016;18:1622–33.
33. Katz AM, Amankulor NM, Pitter K, Helmy K, Squatrito M, Holland EC. Astrocyte-specific expression patterns associated with the PDGF-induced glioma microenvironment. PLoS One 2012;7:e32453.
34. Chekhonin IV, Chistiakov DA, Grinenko NF, Gurina OI. Glioma cell and astrocyte co-cultures as a model to study tumor-tissue interactions: a review of methods. Cell Mol Neurobiol 2018;38:1179–95.
35. Buckingham SC, Robel S. Glutamate and tumor-associated epilepsy: glial cell dysfunction in the peritumoral environment. Neurochem Int 2013;63:696–701.
36. Pallud J, Van Quyen ML, Bielle F, Pellegrino C, Varlet P, Labussiere M, et al. Cortical GABAergic excitation contributes to epileptic activities around human glioma. Sci Transl Med 2014;6:244ra89.
37. Klinger NV, Shah AK, Mittal S. Management of brain tumor-related epilepsy. Neurol India 2017;65:S60–S70.
38. Rao P, Yallapu MM, Sari Y, Fisher PB, Kumar S. Designing novel nanoformulations targeting glutamate transporter excitatory amino acid transporter 2: implications in treating drug addiction. J Pers Nanomed 2015;1:3–9.
39. Pajarillo E, Rizor A, Lee J, Aschner M, Lee E. The role of astrocytic glutamate transporters GLT-1 and GLAST in neurological disorders: Potential targets for neurotherapeutics. Neuropharmacology 2019;161:107559.
40. Buckingham SC, Campbell SL, Haas BR, Montana V, Robel S, Ogunrinu T, et al. Glutamate release by primary brain tumors induces epileptic activity. Nat Med 2011;17:1269–74.
41. Jacobs VL, De Leo JA. Increased glutamate uptake in astrocytes via propentofylline results in increased tumor cell apoptosis using the CNS-1 glioma model. J Neurooncol 2013;114:33–42.
42. MacKenzie G, O'Toole KK, Moss SJ, Maguire J. Compromised GABAergic inhibition contributes to tumor-associated epilepsy. Epilepsy Res 2016;126:185–96.
43. Robel S, Buckingham SC, Boni JL, Campbell SL, Danbolt NC, Riedemann T, et al. Reactive astrogliosis causes the development of spontaneous seizures. J Neurosci 2015;35:3330–45.
44. Untiet V, Kovermann P, Gerkau NJ, Gensch T, Rose CR, Fahlke C. Glutamate transporter-associated anion channels adjust intracellular chloride concentrations during glial maturation. Glia 2017;65:388–400.

Published OnlineFirst May 11, 2020; DOI: 10.1158/1535-7163.MCT-19-0910

Molecular Cancer Therapeutics

Blockade of Cell Volume Regulatory Protein NKCC1 Increases TMZ-Induced Glioma Apoptosis and Reduces Astrogliosis

Lanxin Luo, Xiudong Guan, Gulnaz Begum, et al.

Mol Cancer Ther 2020;19:1550-1561. Published OnlineFirst May 11, 2020.